Supporting Information

Title: A green and facile synthesis of ordered mesoporous nano-silica using coal fly ash

Feng Yan, Jianguo Jiang, Sicong Tian, Zongwen Liu, Jeffrey Shi, Kaimin Li, Xuejing Chen and Yiwen Xu

1. Experimental: Characterization

2. Results:

Table S1. Chemical composition of the coal fly ash and the synthetic nano-silica.

Table S2. Calculation of the Gibbs free energy for Eq. S1-S5.

Table S3. Weight loss, hydroxyl content and hydroxyl density of the synthetic nano-silica.

Table S4. Cell parameters of the synthetic nano-silica.

Figure S1. (a) N_2 physisorption isotherms and (b) pore size distributions of “FA” and “FA-desilication”.

Figure S2. SEM images of (a) “FA”, and (b) ”FA-desilication”. Magnification factor: ×10 000 for (a-b) and ×50 000 for the Insertion of (a-b).

Figure S3. (a) TGA analysis and (b) FTIR spectra of “SiO_2-0.00”, “SiO_2-0.04”, “SiO_2-0.08”, “SiO_2-0.16” and “SiO_2-0.32”.

Figure S4. XRD patterns of “SiO_2-0.00”, “SiO_2-0.04”, “SiO_2-0.08”, “SiO_2-0.16” and “SiO_2-0.32”.

Figure S5. SEM images of (a) “SiO_2-0.00”, (b) “SiO_2-0.08”, (c) “SiO_2-0.16” and (d) “SiO_2-0.32”. Magnification factor: ×10 000 for (a-d) and ×50 000 for the Insertion of (a-d).

Figure S6. Particle size number distribution of “SiO_2-0.00”, “SiO_2-0.04”, “SiO_2-0.08”, “SiO_2-0.16” and “SiO_2-0.32” calculated by DLS method.

1. Experimental

Characterization

The mineral composition of the coal fly ash was recorded using X-ray diffraction (XRD, Rigaku D/max 2500 PC, Japan) with Cu-Kα radiation (λ = 1.5418 Å), and diffraction data were recorded in the 2θ range of 10-80º with a scanning rate of 2º min^{-1}. The small-angle X-ray diffraction (SAXRD), in the 2θ range of 0.6-5º (0.5º min^{-1}), was used to determine the structure of the synthetic nano-silica. Nitrogen adsorption-desorption isotherms of nanoparticles at 77 K were collected on a gas adsorption analyzer (Micrometrics Instrument, ASAP2020, America); all samples were degassed in a vacuum at 90ºC for 1 h and at 350ºC for 4 h before measurement. The specific surface area was calculated using the Brunauer-Emmett-Teller (BET) method over $P \cdot P_0^{-1}$ = 0.05-0.25, and the total pore volume was calculated from the adsorbed volume at $P \cdot P_0^{-1}$ = 0.99. The average pore size and pore distributions were derived from the adsorption branch of the N_2 isotherm using the Barrett-Joyner-Halenda (BJH) method. The size of silica agglomerates and particle size distribution was examined using a nanoparticle size analyzer (Beckman coulter DelsaNano C, America); 0.1 wt. % silica was dispersed in ethanol by ultrasonic waves for 10 min before the measurement. The surface morphology of the samples was observed using a scanning electron microscopy (SEM, Zeiss Merlin Compact, Germany) with a 5-kV electron beam. Transmission electron microscopy (TEM) experiments were conducted on a JEOL JEM-2010F microscope (Japan) operated at 200-kV. The hydroxyl content was calculated using a Thermogravimetric Analyzer (TGA, Mettler-Toledo, TGA/DSC 2, Switzerland) from 25ºC to 1000ºC with a heating rate of 10ºC min^{-1} under nitrogen gas. Fourier-transform infrared (FTIR) spectra were collected on a Fourier spectrometer (Nicolet NEXUS 870, America) using KBr pellets.

2. Results

Table S1. Chemical composition of the coal fly ash and the synthetic nano-silica

Sample	SiO_2 (wt. %)	Al_2O_3 (wt. %)	Fe_2O_3 (wt. %)	Na_2O (wt. %)	CaO (wt. %)	TiO_2 (wt. %)	MgO (wt. %)	K_2O (wt. %)	Residual (wt. %)
FA	52.00	36.51	5.03	0.14	2.61	1.80	0.33	0.77	0.81
FA-5%NaOH [a]	43.39	42.05	5.93	2.19	3.15	1.97	0.39	0.38	0.55
FA-15%NaOH [a]	38.86	44.39	6.50	3.41	3.51	2.10	0.43	0.20	0.60
FA-25%NaOH [a]	34.80	46.92	4.91	6.31	3.39	2.44	0.30	0.10	0.83
FA-35%NaOH [a]	39.35	38.40	6.63	9.50	3.07	1.84	0.37	0.24	0.60
FA-50ºC [b]	47.24	39.78	5.38	0.69	2.99	2.14	0.29	0.82	0.67
FA-70ºC [b]	43.61	42.87	5.62	0.92	3.03	2.32	0.27	0.67	0.69
FA-90ºC [b]	39.37	43.69	5.94	3.29	3.59	2.57	0.37	0.33	0.85
FA-110ºC [b]	34.80	46.92	4.91	6.31	3.39	2.44	0.30	0.10	0.83
FA-130ºC [b]	35.22	45.46	5.04	7.22	3.44	2.38	0.32	0.12	0.80
SiO_2-once [c]	98.35	1.00	0.12	0.25	0.01	N.D. [d]	N.D.	0.16	0.11
SiO_2-0.00	99.29	0.18	0.05	0.28	0.06	N.D.	N.D.	0.10	0.04

[a] The coal fly ash after desilication, the reaction conditions were same with Figure 1b. [b] The coal fly ash after desilication, the reaction conditions were same with Figure 2b. [c] "SiO_2-once" was synthesized via once carbonation while the other conditions were same with "SiO_2-0.00". [d] N.D., not detected.

Table S2. Calculation of the Gibbs free energy for Eq. S1-S5

Equation	ΔH^{Θ} (298.15 K) (kJ mol^{-1})	ΔG^{Θ} (298.15 K) (kJ mol^{-1})	ΔG (323.15 K) (kJ mol^{-1})	ΔG (343.15 K) (kJ mol^{-1})	ΔG (363.15 K) (kJ mol^{-1})	ΔG (383.15 K) (kJ mol^{-1})	ΔG (403.15 K) (kJ mol^{-1})
Eq. S1	37.54	-61.46	-70.14	-77.59	-85.48	-93.77	-102.45
Eq. S2	44.75	-55.79	-64.60	-72.15	-80.14	-88.54	-97.32
Eq. S3	-11.78	-2.32	-1.71	-1.47	-1.44	-1.60	-1.95
Eq. S4	24.86	322.93	346.63	363.80	379.50	393.80	406.76
Eq. S5	-324.48	-559.14	-577.41	-590.10	-601.19	-610.76	-618.90

$$SiO_{2(Amorphous)}+2OH^-_{(aq)} \rightarrow SiO_3{}^{2-}{}_{(aq)}+H_2O_{(l)} \quad \text{(Eq. S1)}$$

$$SiO_{2(Quartz)}+2OH^-_{(aq)} \rightarrow SiO_3{}^{2-}{}_{(aq)}+H_2O_{(l)} \quad \text{(Eq. S2)}$$

$$Al_2O_{3(Corundum)}+2OH^-_{(aq)}+3H_2O_{(l)} \rightarrow 2Al(OH)_4{}^-{}_{(aq)} \quad \text{(Eq. S3)}$$

$$Al_6Si_2O_{13(Mulite)}+10OH^-_{(aq)}+7H_2O_{(l)} \rightarrow 6Al(OH)_4{}^-{}_{(aq)}+2SiO_3{}^{2-}{}_{(aq)} \quad \text{(Eq. S4)}$$

$$6Al(OH)_4{}^-{}_{(aq)}+6SiO_3{}^{2-}{}_{(aq)}+8Na^+_{(aq)} \rightarrow Na_8Al_6Si_6O_{24}(OH)_2(H_2O)_{2(s)}+4H_2O_{(l)}+10OH^-_{(aq)} \quad \text{(Eq. S5)}$$

Table S3. Weight loss, hydroxyl content and hydroxyl density of the synthetic nano-silica

Sample	Weight loss (wt. %)				N_{OH} [a] (mmol g^{-1})	C_{OH} [b] (OH nm^{-2})
	25-200ºC	200-600ºC	600-1000ºC	Total		
SiO_2-0.00	2.91	4.02	0.63	7.55	5.16	10.75
SiO_2-0.04	1.93	0.83	0.96	3.72	1.99	2.97
SiO_2-0.08	1.03	0.57	1.85	3.44	2.68	2.04
SiO_2-0.16	0.59	0.34	1.88	2.80	2.46	1.28
SiO_2-0.32	0.92	0.26	1.76	2.95	2.25	1.28

[a] N_{OH}, hydroxyl content; [b] C_{OH}, hydroxyl density.

Table S4. Cell parameters of the synthetic nano-silica

Sample	$2\theta_{100}$ (º)	$2\theta_{110}$ (º)	$2\theta_{200}$ (º)	d_{100} (Å) [a]	d_{110} (Å)	d_{200} (Å)	a_0 (nm) [b]
SiO_2-0.00	N.A. [c]	N.A.	N.A.	N.A.	N.A.	N.A.	N.A.
SiO_2-0.04	2.580	4.379	N.D.	34.21	20.16	N.D.	3.95
SiO_2-0.08	2.480	4.261	N.D.	35.59	20.72	N.D.	4.11
SiO_2-0.16	2.370	4.020	4.639	37.25	21.96	19.03	4.30
SiO_2-0.32	2.361	4.039	4.639	37.39	21.86	19.03	4.32

[a] d_{100}, interplanar spacing of the (1 0 0) reflection, which was obtained from the diffraction peak (1 0 0) by the Bragg's Law, $2 \times d_{100} \times \sin\theta_{100} = \lambda$; [b] a_0, hexagonal unit cell parameter, which is calculated by $a_0 = 2 \times d_{100} / \sqrt{3}$; [c] N.A., not available.

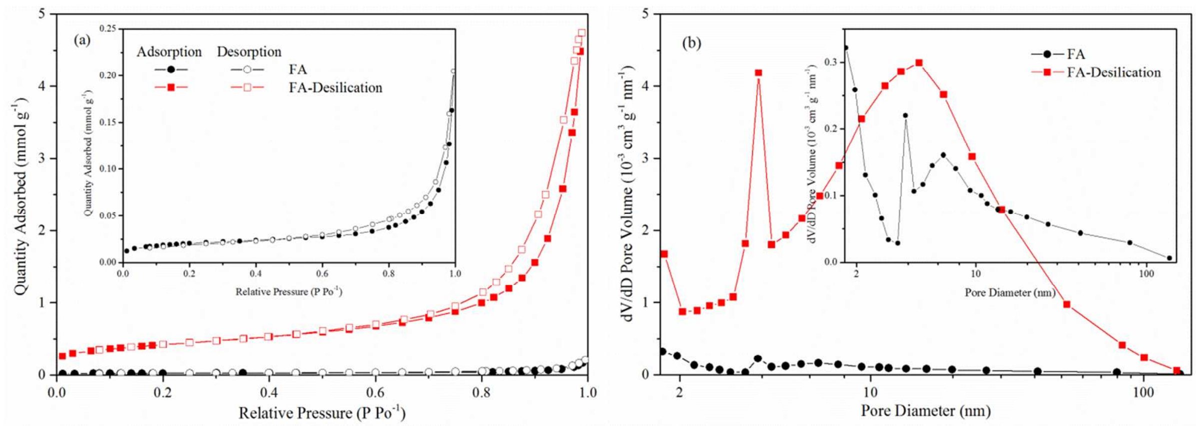

Figure S1. (a) N_2 physisorption isotherms and (b) pore size distributions of "FA" and "FA-desilication".

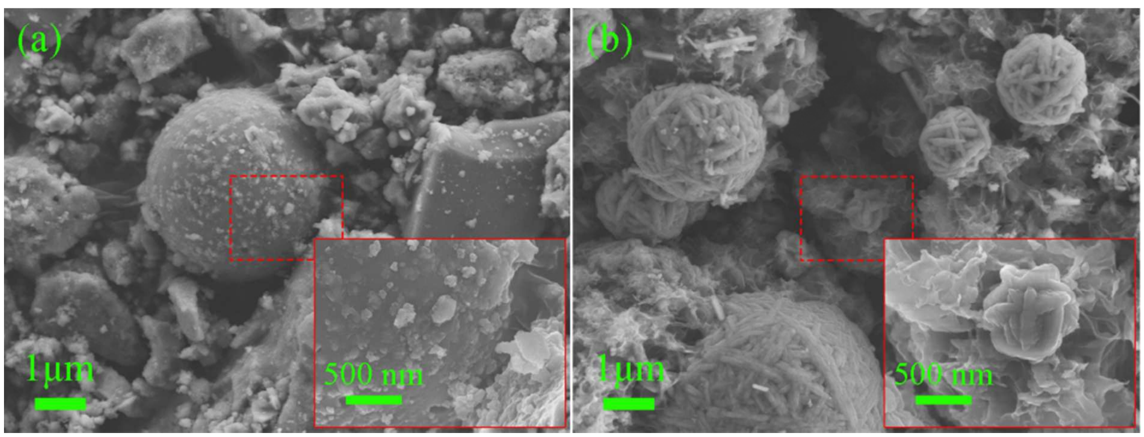

Figure S2. SEM images of (a) "FA", and (b) "FA-desilication". Magnification factor: ×10 000 for (a-b) and ×50 000 for the Insertion of (a-b).

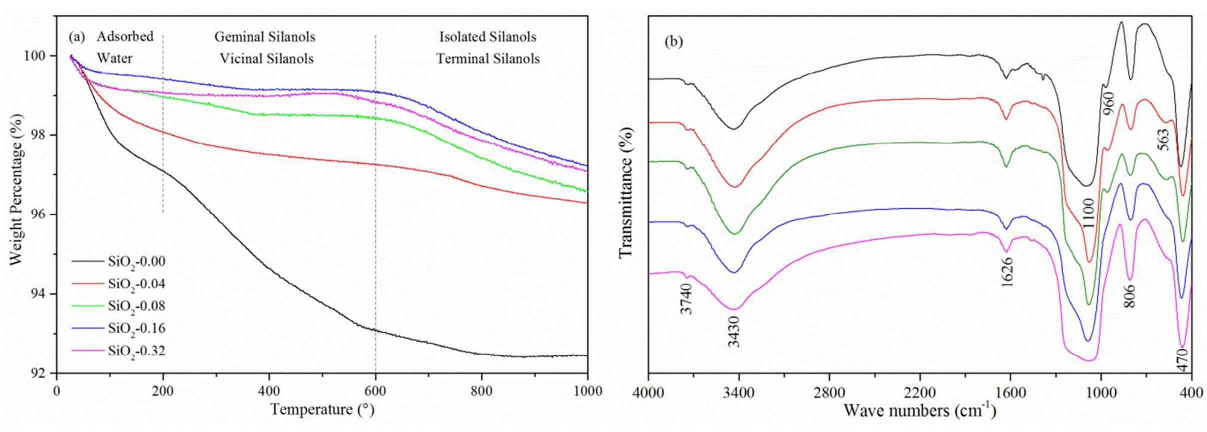

Figure S3. (a) TGA analysis and (b) FTIR spectra of "SiO_2-0.00", "SiO_2-0.04", "SiO_2-0.08", "SiO_2-0.16" and "SiO_2-0.32".

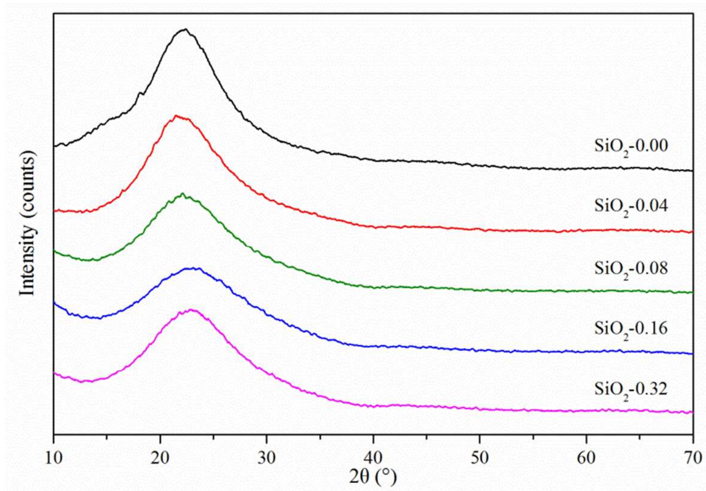

Figure S4. XRD patterns of “SiO_2-0.00”, “SiO_2-0.04”, “SiO_2-0.08”, “SiO_2-0.16” and “SiO_2-0.32”.

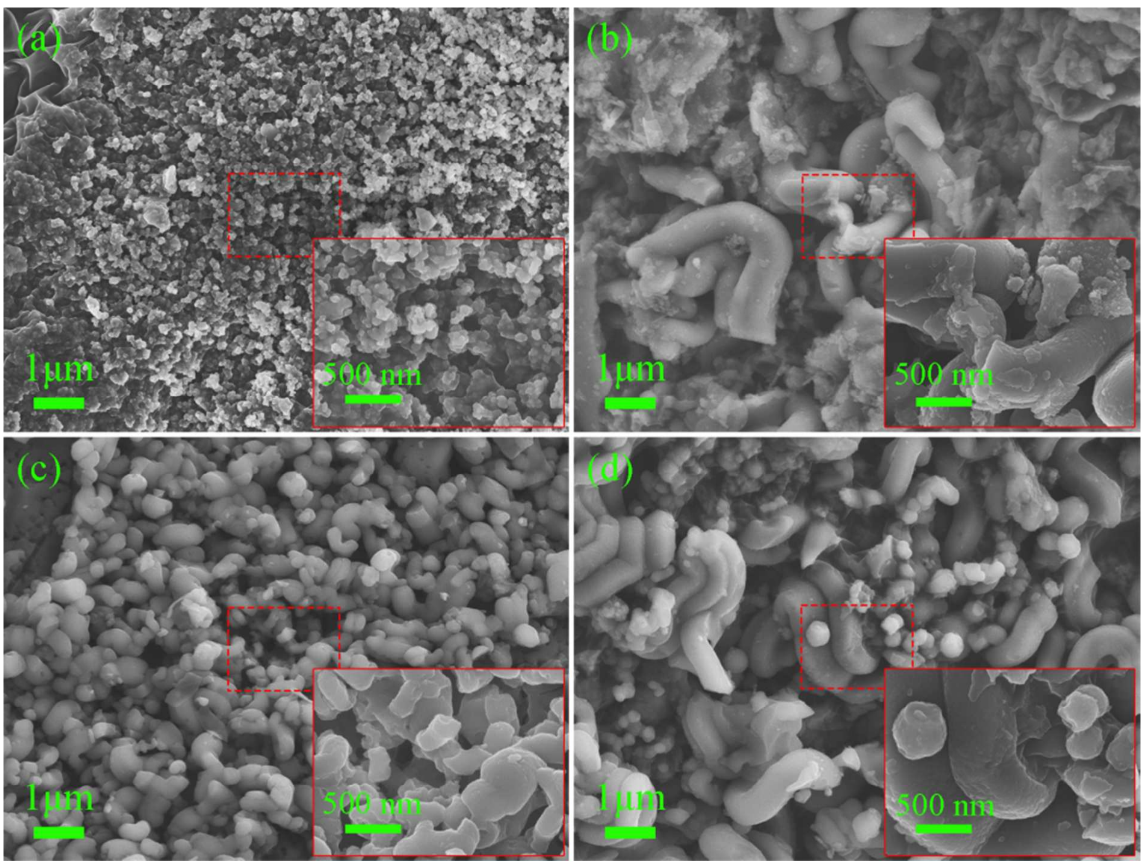

Figure S5. SEM images of (a) “SiO_2-0.00”, (b) “SiO_2-0.08”, (c) “SiO_2-0.16” and (d) “SiO_2-0.32”. Magnification factor: ×10 000 for (a-d) and ×50 000 for the Insertion of (a-d).

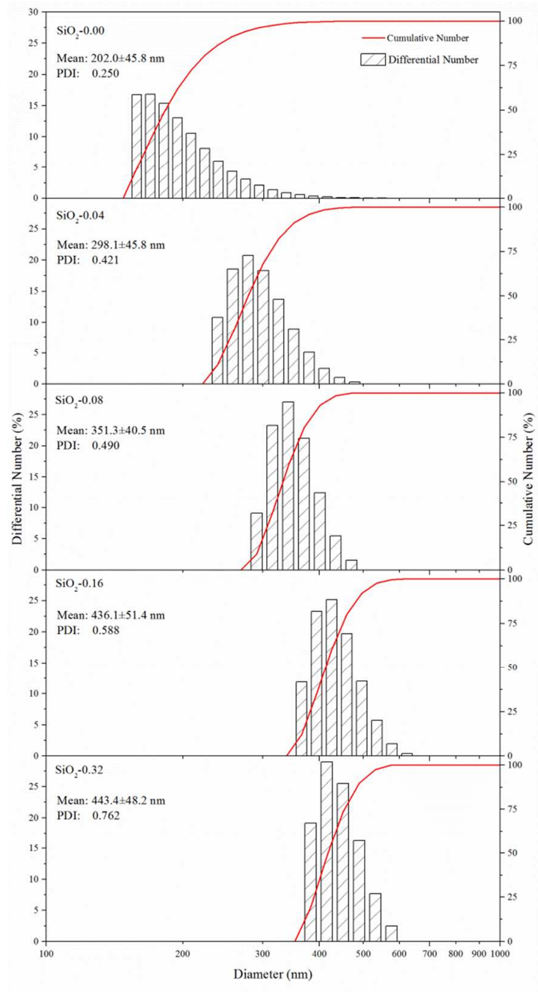

Figure S6. Particle size number distribution of "SiO_2-0.00", "SiO_2-0.04", "SiO_2-0.08", "SiO_2-0.16", and "SiO_2-0.32" calculated by DLS method.